Geophysical Studies of the Raahe-Ladoga Shear Complex in the Iisalmi Area of Finland

Mohamed Abdel Zaher[1][*][,2], Markku Pirttijärvi[2] and Toivo Korja[3,4]

[1]National Research Institute of Astronomy and Geophysics (NRIAG)
[2]Department of Physics, University of Oulu
[3]Oulu Mining School, University of Oulu
[4]Geosciences and Environmental Engineering, Luleå University of Technology
*Corresponding author, e-mail: moh_zaher@yahoo.com

Abstract

We have studied geophysical properties of the Raahe-Ladoga Shear Complex, a major NW-SE trending strike-slip shear zone in Central Finland. Aeromagnetic and airborne electromagnetic data from the Raahe-Ladoga Shear Complex, provided by the Geological Survey of Finland, were processed and interpreted in combination with the regional gravity data of the Finnish Geodetic Institute and the Geological Survey of Finland. Filtering techniques such as the first vertical derivative, horizontal and tilt gradients, and pseudo-gravity were applied for the visual interpretation and analyses of the shear complex in the Iisalmi area. The gravity data emphasized a NW-SE trend along a transition zone between the Archaean Karelian Province and the Palaeoproterozoic Svecofennian Province. This is consistent with the anomalies in the magnetic field intensity. Geophysical properties were also studied with gravity, magnetic and magnetotelluric ground surveys that were conducted across a narrow dominant segment of the entire shear complex near Iisalmi. The data indicated that weak negative gravity anomalies and strong magnetic anomalies are associated with the shear zone. Gravity modelling suggests that anomalies of small wavelength are related to shear zones and fractures, but the depth extent and dip cannot be resolved. Magnetic interpretation revealed that the shear zone can be modelled with near-vertical (82° eastward dip) sheet-like bodies with a depth extent over 2 km. The 2-D inversion of magnetotelluric data shows that the upper crust in the Iisalmi area is very resistive. High resistivity of the strongly sheared crust suggests the old shear complexes are not necessarily conductive opposite to many active shear complexes worldwide.

Keywords: gravity, magnetics, magnetotellurics, airborne surveys, ground surveys, shear zone, Fennoscandian Shield, Raahe-Ladoga Shear Complex, Iisalmi

1   Introduction

The orogenic evolution has in general three distinct phases, (1) the construction of a crustal accretionary wedge in subdduction, (2) the development of a continental plateau, and (3) gravitational collapse – each of which will leave different tectonic and magmatic markers (*Beaumont et al.,* 2001; *Vanderhaeghe and Teyssier*, 2001a,b) and consequently distinct geophysical signatures such as regions of enhanced electrical conductivity due to partial melt or graphite and/or sulphides of metasedimentary rock assemblages deposited in various basin environments (e.g. *Unsworth*, 2009; *Korja*, 2007;

Neska, 2016). It should be noted that our present day geophysical observations do not distinguish different geological processes as such that are responsible for geophysical structure but have signatures from the entire tectonic evolution of subsurface. One of the tasks in interpretation is to distinguish the traces of different processes. To better constrain the processes, observational data are needed from deeper orogenic crustal sections exposed in the ancient orogens, such as the Precambrian Svecofennian Orogen in the Fennoscandian Shield. In addition to deep exhumation levels of the frozen structure, the shields also offer observations on how and why the process became extinct and what are the end products.

The Svecofennian Province is a typical granite-gneiss terrane that represents 15-20 km deep section through an evolved orogen. It is a part of a larger orogenic system associated with the construction of the Columbia supercontinent (*Zhao et al.*, 2004). Similarly, to Alpine systems, the Svecofennian orogenic system consists of accreted arc terranes and intervening basins at an older continental margin and has been evolved through many stages including subduction, oblique collision and post-collisional extension (*Gaal and Gorbatschev*, 1987; *Ekdahl*, 1993; *Korsman et al.*, 1999; *Koistinen et al.*, 2001; *Lahtinen et al*, 2005; *Korja A. et al.*, 2006).

The study area is in central Finland, where the Keitele microcontinent in southwest and intervening basins and arcs accreted to continental plate, viz. Karelia in northeast, at around 1900 Ga and formed the core of the Svecofennian orogen (*Lahtinen et al.*, 2005; *Korja A. et al.*, 2009). Because the convergence between Keitele and Karelia was oblique, large strike slip faults developed along the Keitele margin.

The Raahe–Ladoga Shear Complex (RLSC) represents a major, c. 100 km wide, NW-SE trending system of vertical shear zones, wrench faults and intervening crustal blocks in the central part of the Fennoscandian Shield (*Woodard et al.*, 2015). It separates the partly reworked Archaean Karelia Craton and folded and metamorphosed Palaeoproterozoic (ca. 2.5-2.0 Ga) cover sequences in the NE from the ca. 1.93-1.87 Ga old Svecofennian arc complexes in the SW (*Gaal and Gorbatschev*, 1987; *Korsman et al.*, 1999; *Woodard et al.*, 2015). RLSC is characterized by strongly sheared rocks and intervening crustal blocks in which earlier structures are preserved (Fig. 1). The Keitele, Pielavesi, and Savonranta shear zones are the most important shear-dominated units of the RLSC (Fig. 1) that were formed by long-term and multi-phase Svecofennian convergent tectonic evolution. The zone has been active at several stages and records deformation and associated magmatism at different depths. It is an example on deep level process at major strike slip fault and/or continental transform boundary or transfer shear zone such as San Andreas or Altyn Tagh faults. Lithologically the study area (Fig. 1) consists mainly of over 2500 Ma old Archaean tonalitic migmatites (*Paavola,* 1991) and of Proterozoic supracrustal paragneisses and intrusive rocks in the western part of the study area. The NW-SE trending RLSC forms a major ore-bearing district along the Archaean-Proterozoic boundary.

We present the results of the analysis and processing of high-resolution low-altitude airborne geophysical data in combination with regional gravity data to study the properties of RLSC in the Iisalmi area. Filtering techniques such as the first vertical de-

rivative, pseudo-gravity, tilt gradient, and horizontal gradient were applied to delineate the geological structures in the study area. The airborne geophysical data including aeromagnetic and electromagnetic maps were used to examine lateral changes in magnetic susceptibilities and apparent resistivities at critical depths. As a part of MIDCRUST project (*Korja, A. et al,* 2012), ground gravity and magnetic surveys were conducted along two profiles spaced approximately 5 km apart crossing a shear zone near Iisalmi (Fig. 2). The purpose of these surveys was to use the gravity and magnetic data to infer changes in the subsurface density and magnetic susceptibility that can be related to the lithology and the intensity of the shear zones. Gravity and magnetic data were interpreted using 2.5-D density and susceptibility models with the help of petrophysical density and magnetic susceptibility data determined for the rock samples collected in the study area. The device designed by the GTK (*Puranen et al.,* 1968; *Puranen and Sulkanen*, 1985) was used for measurements. Additionally, broadband MT soundings were carried out in the study area to investigate electrical conductivity structure across the Archaean-Proterozoic boundary. The MT profile (MT-MT*) is collocated with the gravity profile GA-GA* passing through main shear zones in the Iisalmi area (Fig. 2).
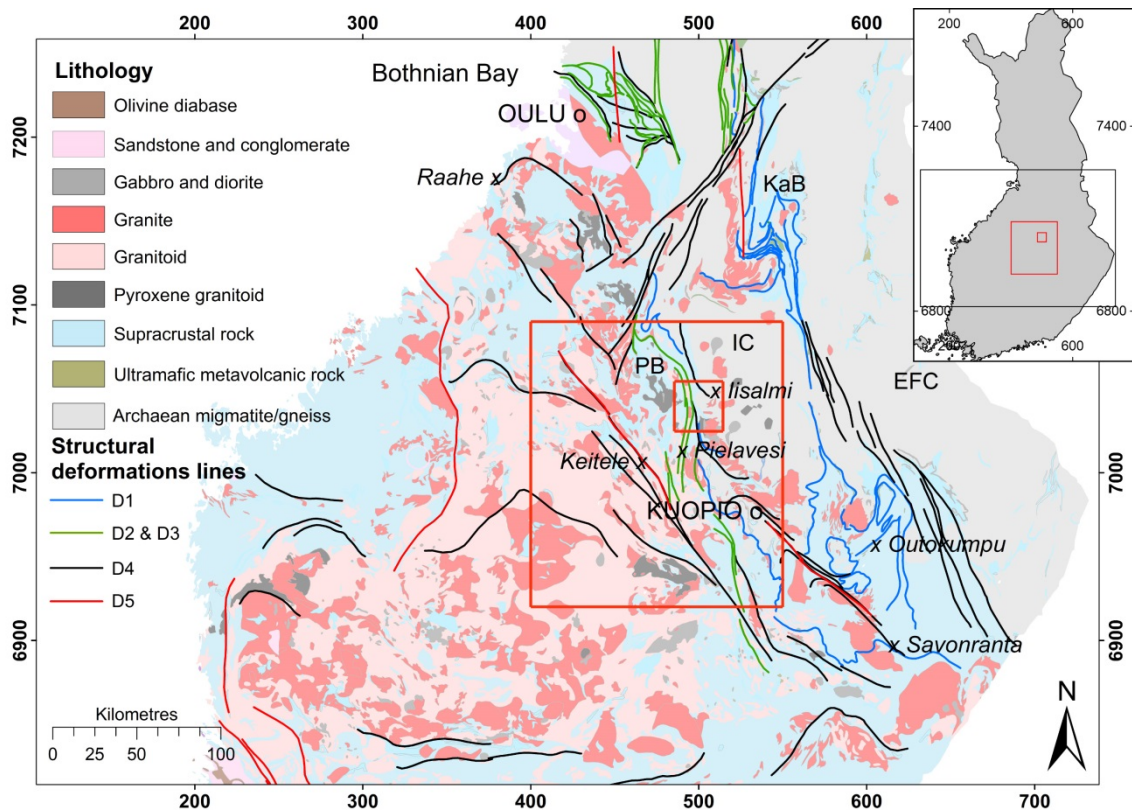

Fig. 1. Simplified geological map of Finland derived from the map in a scale of 1:200000 © Geological Survey of Finland 2013. Structural deformation lines (D1-D5) are from *Kärki et al.* (1993). Two red rectangles show the locations of maps in Figs. 2–7. Coordinates (ETRS89-TM35FIN) in this figure, and in all subsequent figures, are in kilometres. EFC=Eastern Finland Complex; IC=Iisalmi Complex; KaB=Kainuu Belt; PB=Pyhäsalmi Belt.
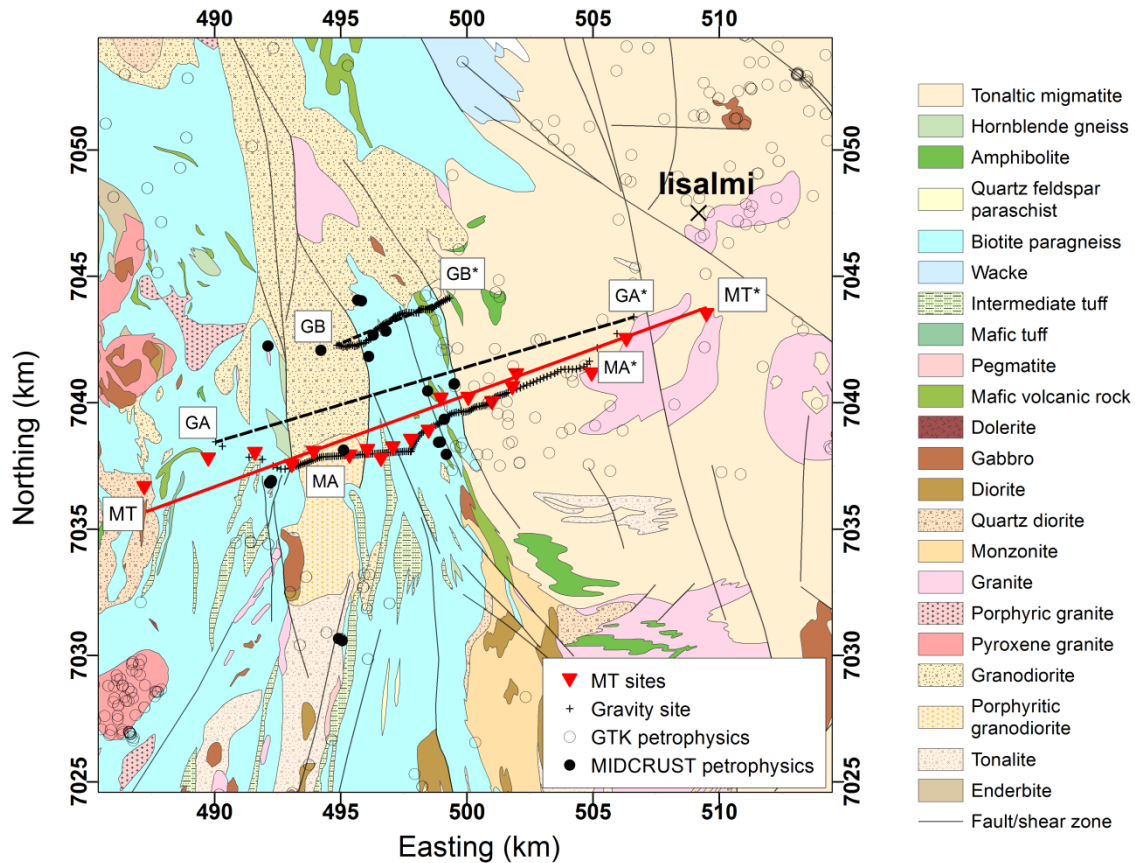
Fig. 2. Geophysical measurements in the study area: gravity and magnetotelluric sites and the location of the petrophysical samples. Dashed black lines (GA-GA* and GB-GB*) and solid red line (MT-MT*) represent gravity and magnetotelluric model profiles, respectively. MA and MA* denote the start and end of magnetic line, which coincides with the gravity line GA-GA* but is shorter. Background map is the geological map of Finland in a scale of 1:200000 © Geological Survey of Finland 2013.

2   Previous geophysical studies

There are several geophysical data sets that have been used to explore the deep structure of the RLSC. Deep seismic sounding data in the Fennoscandian Shield show marked crustal thickness variations along RLSC: in SE, in the Outokumpu region (Fig. 1), the crust is over 60 km thick whereas in NW, in the Bothnian Bay, it is c. 40-45 km thick (*Luosto*, 1991; *Korja, A. et al.*, 1993; *Grad et al.,* 2009). Lateral crustal thickness variations are primarily due to thickness variations of lower crustal high velocity layer *(Korja, A., et al.,* 1993). More detailed geophysical information is available from several profiles crossing RLSC. Two FIRE seismic reflection profiles (*Kukkonen and Lahtinen*, 2006) cross RLSC: one in the Outokumpu area and another in the Kainuu area c. 35 km to the north from our study area. In the latter, the seismic sections contain features (e.g. breaks in sub-horizontal reflectors) that suggest deep, sub-vertical shear zones (*Korja, A. et al.*, 2006). Magnetotelluric (MT) GGTSVEKA profile (*Korja and Koivukoski*, 1994*; Lahti et al.,* 2002) crosses RLSC in our study area. The site distance of GGTSVEKA profile in this area is over 10 km, which hampers near-surface investigations but provides information on deeper structures in the vicinity of our study area.

Later *Vaittinen et al.* (2012) obtained three 2-D conductivity models across the Archaean-Proterozoic boundary to north and north-east of our study area. They identified two major sets of crustal conductors, which have opposite dip to west and east. The westward dipping conductors in the east mark Palaeoproterozoic conductive metasediments of the Kainuu Belt (KaB) between two Archaean (IC and EFC) units whereas eastward dipping conductors mark conductive metasediments of the PB (Fig. 1). The third MT-profile crosses RLSC next to the Bothnian Bay (Oulu I profile, *Korja et al.*, 1986) and the model from this study suggests that the conductive Palaeoproterozoic metasedimentary rocks on the Archaean Karelian craton margin extend south-westward under the Svecofennian rocks.

The regional gravity data (Fig. 3a) are from the Bouguer anomaly map of Fennoscandia (*Korhonen et al.,* 2002a). Correlation of the Bouguer anomaly map with the geological data shows distinct Bouguer anomaly maxima associated with greenstone and metavolcanic rocks, and schist and migmatite belts when surrounded by low-density granites. Large gravity minima are associated with the Archaean basement, which have lower density than their surroundings. The RLSC is imaged on a Bouguer anomaly map by narrow linear lows running NW-SE, indicating low density caused by fractured and/or weathered fault zones.

Low- and high-altitude airborne geophysical data from the Geological Survey of Finland (GTK) are very valuable data to study the detailed structural properties of RLSC as described, in general, by many authors (e.g., *Poikonen et al.*, 1998; *Peltoniemi,* 2005; *Airo,* 2005; *Leväniemi et al.*, 2009). *Lanne et al.* (1998, 2002) described the use of airborne magnetic data to locate fracturing in the crystalline bedrock. The map in Fig. 3b represents anomalous magnetic field from high-altitude (150 m) data after subtracting Earth's main field. Regional geological and structural features can be seen from the high-altitude magnetic data. Magnetic highs (up to 500 nT) are associated with rocks that have higher magnetic susceptibility than the surroundings rocks. The RLSC is characterized by diverse magnetic anomalies and the zone does not appear in magnetic maps as clearly as in Bouguer anomaly maps. In some parts, the negative magnetic anomalies suggest that the magnetic susceptibility has been destroyed during the shearing process.

3   Existing geophysical data used in the study

To get more detailed information out from the existing datasets, the low-altitude magnetic data and the Bouguer data were processed using 2-D Fourier transform methods by the FOURPOT software developed by *Pirttijärvi* (2012). The magnetic and gravity anomaly patterns of the processed maps were used to indicate the presence of faults and shear zones in the study area.
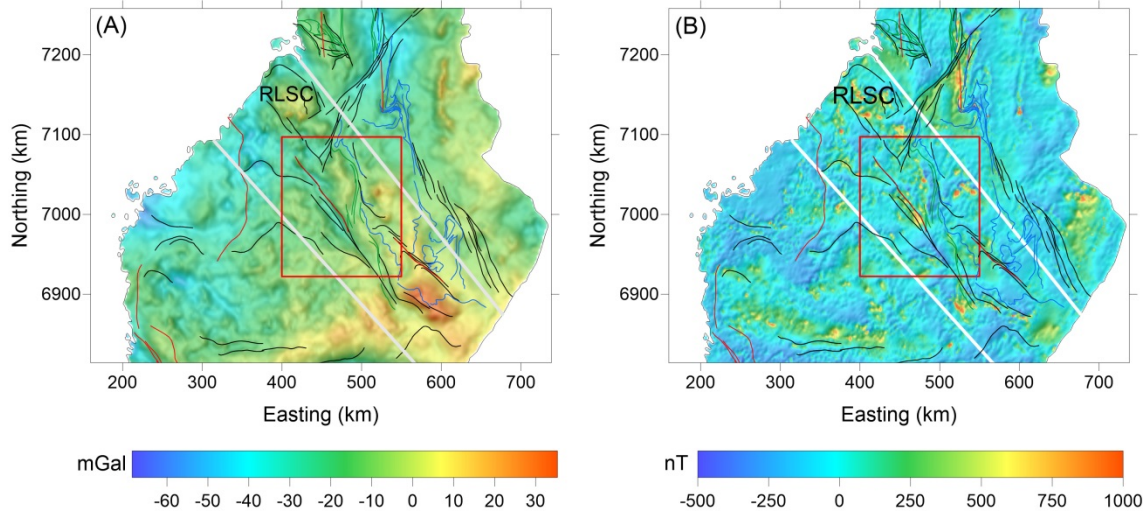
Fig. 3. The location of the Raahe-Ladoga Shear Complex (RLSC) in Central Finland outlined by white lines. The background geophysical maps are (A) regional Bouguer anomaly map (*Korhonen et al.*, 2002a) and (B) high-altitude aeromagnetic anomaly map (*Korhonen et al.*, 2002b). The red rectangle outlines the area of the maps in Fig. 4. The structural deformation lines (D1-D5) from Fig. 1 are overprinted in maps.

3.1   *Bouguer anomaly data*

The regional gravity data of Iisalmi were based on the Fennoscandian Bouguer anomaly map of GTK (*Korhonen et al.,* 2002a) defined on a 2.5 km by 2.5 km grid. Fig. 4a shows the Bouguer anomaly map of the RLSC with all wavelengths greater than 7 km. The gravity anomaly values for the study area range from –25 to 40 mGal. The most significant feature is the intense NW-SE directed negative gravity minimum associated with the RLSC. Such gravity anomaly patterns show a decrease in the bedrock density which often delineates fractured shear zones. Visual inspection of the gravity map shows a positive anomaly eastward, consistent with the existence of a mafic body at a shallow depth. The vertical and horizontal gradient of the Bouguer data are shown in Figs. 4b, 4c to enhance small details related to geological structures. The vertical gradient focuses and narrows the broad gravity anomalies over the sources (Fig. 4b). The horizontal gradient isolates gravity sources and identifies contacts between the lithological units (Fig. 4c). The horizontal gradient can also be used to estimate the dip direction of the contacts and bodies.

The tilt gradient of the Bouguer anomaly map is shown in Fig. 4d. The tilt gradient is the ratio of the vertical gradient and the total horizontal gradient of the gravity field. The tilt gradient map also delineates lithological contacts involving the identification and mapping of the edges of shear zones. Linear features with a NW-SE striking trend are pronounced in the tilt gradient map. The processed maps show a good correlation between linear gravity anomalies and the structural lines of geological maps.
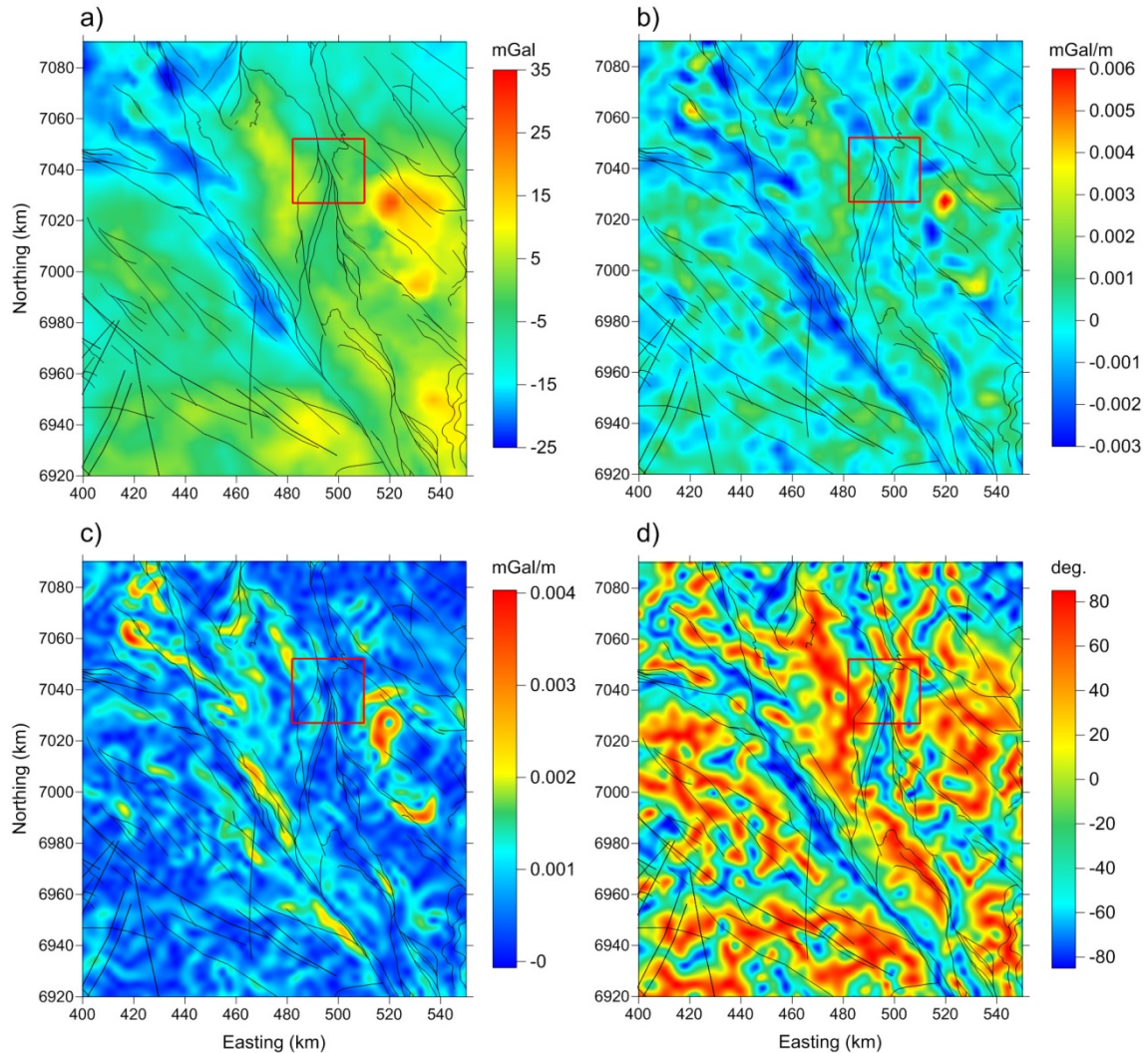
Fig. 4. The derivative maps of the Bouguer anomaly map by *Korhonen et al*. (2002a) interpolated on a 500 x 500 m grid: a) low-pass filtered (7 km) Bouguer anomaly data, b) the first vertical gradient, c) horizontal gradient, and d) tilt gradient (see description in the text). Black lines represent the structural lines taken from the geological map on scale 1:1 million © Geological Survey of Finland 2009. Red rectangular represents the location of the study area shown in Figs. 5–7.

3.2   Aeromagnetic data

Aeromagnetic data are widely used to map and to delineate the subsurface structural faults that affect the basement and overlying sedimentary cover; in our case, mainly post-glacial overburden. The high-altitude data (Fig. 2b) have a nominal ground clearance of 150 m and a line spacing of 400 m and the low-altitude data (Fig. 5) 30 m and 200 m, respectively (*Hautaniemi et al.,* 2005). Flight direction was either north-south or east-west, depending on the main geological trend of the survey area.

Processed low-altitude aeromagnetic maps based on 50 m grid sampling are often detailed enough for structural analysis at different scales. Post-processing with Fourier transform operations provides more information about the subsurface geological structures in the study areas. These transformations make features of particular interest more noticeable to the detriment of others thus helping to correlate the measured field to rock properties.

The aeromagnetic map of the study area provides insights of anomalous magnetic sources after subtracting the Earth's main field. The first stages in the processing of magnetic data are low-pass filtering and reduction to the pole (RTP), a technique that reduces the effect of inclined incident magnetic field (Fig. 5a). This helps to estimate the true dip and strike directions of the targets. The intensity of the magnetic field is controlled by the amount of magnetic minerals in rocks with high magnetic susceptibility (*Telford et al.,* 1978). The aeromagnetic map has proved to be very useful for the delineation of lithologies and structures, and in general there is a very clear correlation between observed surface geology and the aeromagnetic anomaly patterns (see e.g. *Airo,* 1999, 2005 and Airo et al., 2014). The magnetic anomalies of the Iisalmi area are a part of a broader zone of NW-trending anomalies that coincide with the structural lines of the RLSC (Fig. 1). Alteration due to rainfall and runoff causes precipitation of magnetic minerals paralleling the general strike of the shear zone and produces linear magnetic anomalies.

Linear and bended features and the distribution of magnetic anomalies can be clearly observed on mapping the first vertical gradient of the RTP magnetic data (Fig. 5b). Horizontal and tilt gradient maps of the reduced-to-pole aeromagnetic data (Fig. 5c, d) show additional small-scale features, which were not previously recognized. For example, the edges and contacts are enhanced and became more obvious. The NW-SE trending of the linear features are more common in the Iisalmi area, where the linear features follow the structural trend of the RLSC.

To reduce the large amount of details in the magnetic data, a pseudo-gravity transform was applied to the aeromagnetic data. This operation enhances the anomalies associated with deep magnetic sources at the expense of the dominating shallow magnetic sources. The gravity and magnetic fields of a common source of magnetization and the density contrast are related to each other through Poisson's relation and they can be transformed from one to another using Fourier transform methods (*Blakely,* 1995). The pseudo-gravimetric field enhances the anomalies associated with deep magnetic sources and reduces the effect of shallow sources. The pseudo-gravimetric field depends on rock density contrast and magnetization intensity, the latter of which is in turn a function of magnetic susceptibility and the intensity of the inducing magnetic field. We gave for the density contrast, magnetic susceptibility, and geomagnetic field the values of 0.1 g/cm^3, 0.01 SI, and 52500 nT, respectively. The density and susceptibility values were based on a moderate contrast between the different rocks in the study area. The application of horizontal, vertical and tilt gradients on the pseudo-gravimetric field enhances the subtle features and delineate the structures in the study area (Fig. 6b, c, d) with far less amount of details as in the maps derived from the RTP data (Fig. 5).
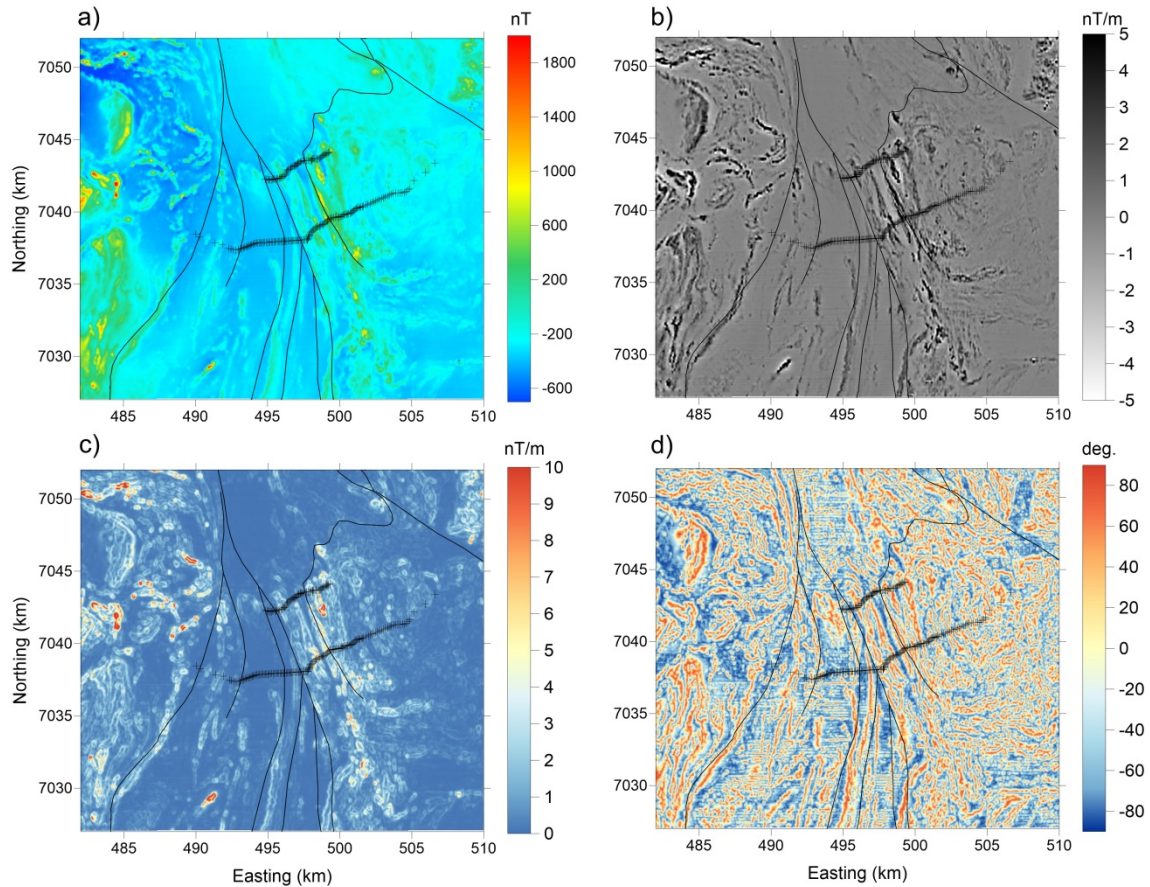
Fig. 5. The derivative maps of the aeromagnetic data from the Geological Survey of Finland (GTK). Data are reduced to pole (RTP data). Maps: a) low-pass filtered (7 km) aeromagnetic data, b) the first vertical gradient, c) horizontal gradient and d) tilt gradient (see description in the text). Black thin lines represent the structural lines taken from the 1:1 million geological map © Geological Survey of Finland 2009. Crosses represent gravity sites.

3.3   Airborne electromagnetic data

Airborne electromagnetic methods (AEM; so-called wing-tip slingram) give information on the electrical conductivity variations from the surface to the depths of a few tens of metres depending on the subsurface conductivity and frequency used. Electrical conductivity, or its reciprocal resistivity, is related to both overburden features such as lake-waters, swamps, sediment layers and bedrock features such as black shales, sulphides and other mineralisations and well as to ground water in bedrock aquifers. The AEM system used in low-altitude mapping of GTK has been described by *Peltoniemi* (1982, 2005), *Poikonen et al.* (1998), and *Hautaniemi et al.* (2005). During the three decades of low-altitude mapping, the AEM system has changed several times. Most importantly, the coaxial system was changed into coplanar 'wing-tip system in 1980 while the frequency remained at roughly 3100 Hz. The GTK AEM system can give information on the conductivity (or resistivity) down to a few tens of metres below the surface.
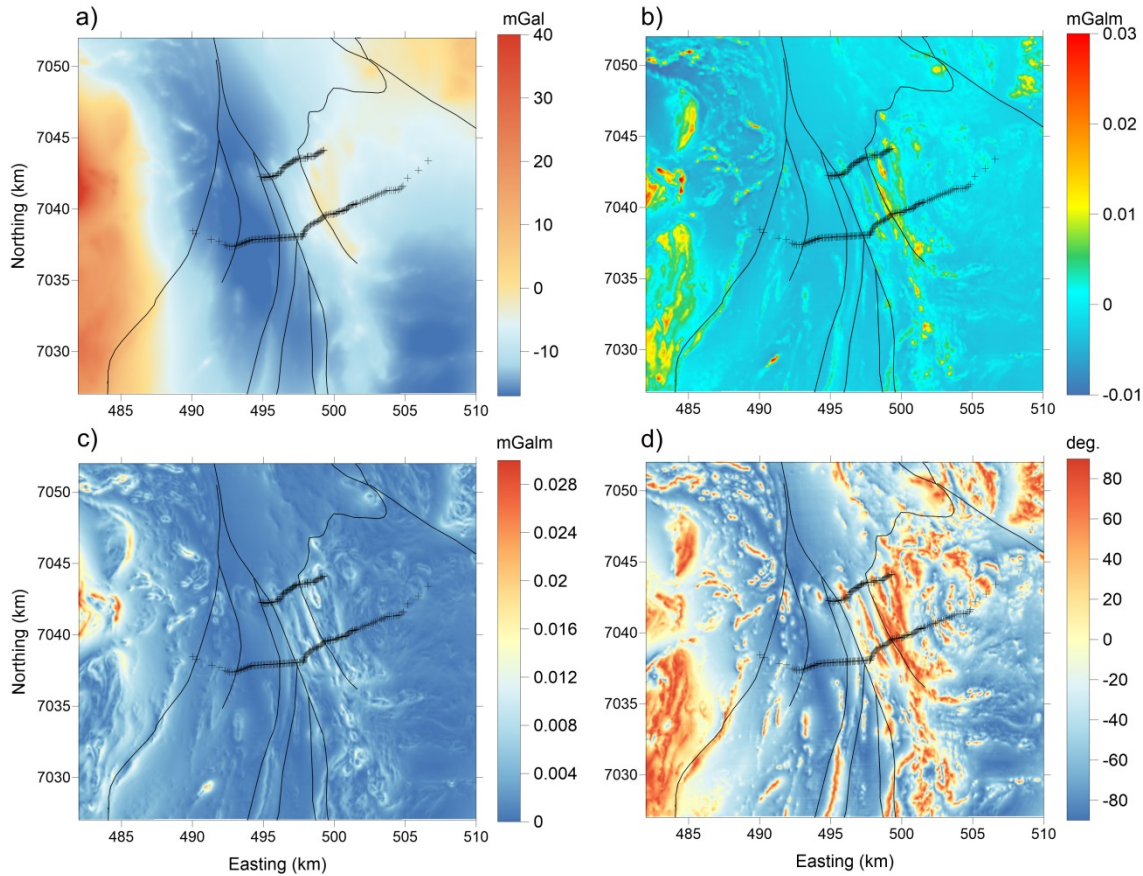
Fig. 6. Pseudo-gravimetric maps of the study area obtained from the aeromagnetic data from GTK. Maps: a) the map of the pseudo-gravimetric field and b) the first vertical gradient, c) the horizontal gradient and d) the tilt gradient of the pseudo-gravimetric field (see description in the text). The pseudo-gravimetric field was computed using density the contrast of 100 kg/m^3 and magnetic susceptibility of 0.01 SI. Local geomagnetic field intensity of 52500 nT, inclination of 75.3° and declination of 9.8° were set for calculation. Black lines represent the structural lines taken from the 1:1 million geological map © Geological Survey of Finland 2009. Crosses represent gravity sites forming two EW-directed profiles.

The apparent resistivity (Fig. 7d) was calculated by Pirttijärvi et al. (2014) on the basis of two-layer combined inversion of the in-phase and out-of-phase (quadrature) components of the AEM data (Fig. 7b, c) and static magnetic field data (Fig. 7a). Resistive areas associated with high magnetic anomalies due to their high magnetite content (Fig. 7a) correspond with the negative values of the in-phase component of the AEM data. Instead of using a conductive half-space model, the apparent resistivity of the basement (Fig. 7d) was calculated by the joint inversion of airborne electromagnetic and magnetic data (Pirttijärvi et al., 2014) where the negative values of the in-phase component are modelled appropriately. Fig. 7d shows that the study area is quite resistive as a whole. Conductive linear anomalies break in locations that are associated with deeper weathering along the shear zones. Western part, and the northwestern part of the study area, in particular, are characterized by higher conductivities that can be associated with graphite and/or sulphide-bearing shear zones.
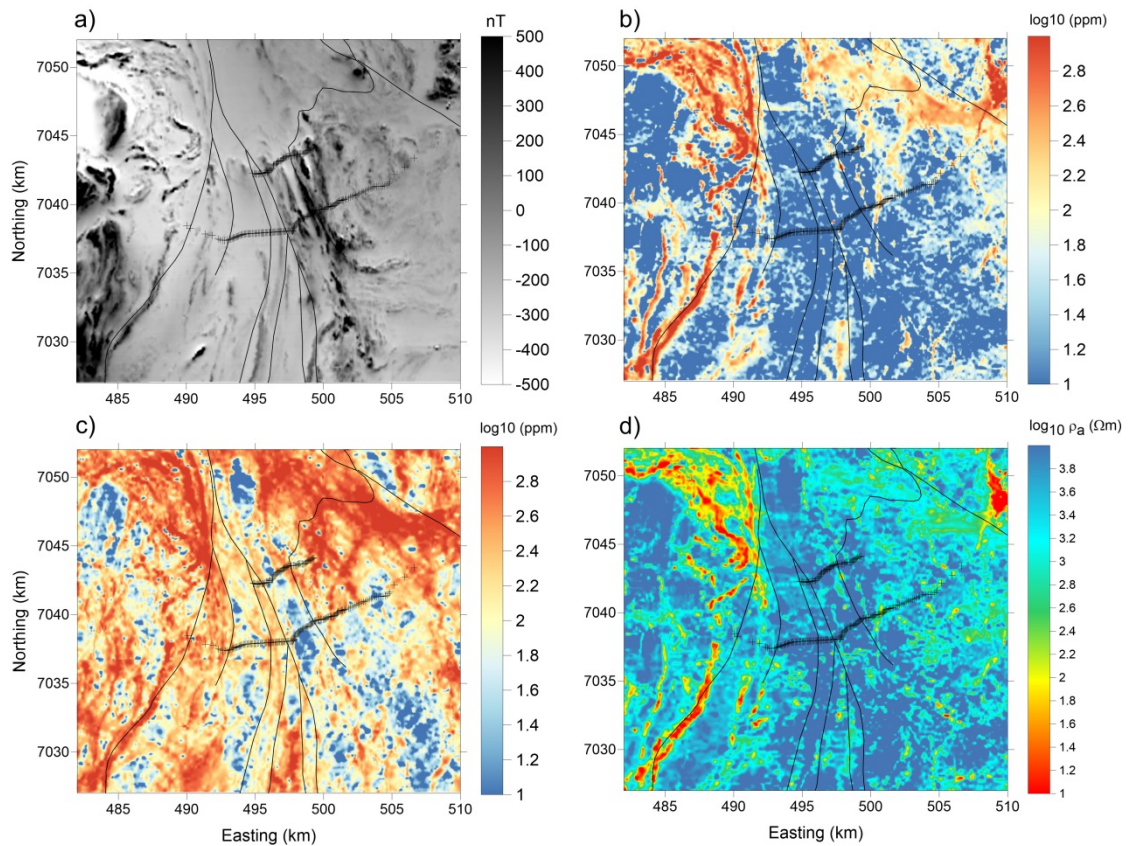
Fig. 7. Geophysical maps of the study area obtained from airborne geophysical (GTK) measurements. Magnetic data were reduced to pole (RTP) prior to the derivation of maps. a) A grayscale map of the aeromagnetic data, b) in-phase electromagnetic data, c) out-of-phase (quadrature) electromagnetic data and d) the apparent resistivity of the basement calculated by the joint inversion of airborne electromagnetic and magnetic data (*Pirttijärvi et al.*, 2014). Black lines represent the structural lines taken from the 1:1 million geological map © Geological Survey of Finland 2009. Crosses represent gravity sites forming two EW-directed profiles.

4   Field surveys

Gravity data were collected along two lines approximately 5 km apart (see Fig. 2). Line A is 16 km long having 147 measurement sites, whereas line B is about 6 km long having 64 sites. Except for the ends of the line A, the station spacing is about 100 m on both lines. Gravity measurements were done using a Scintrex CG-5 Autograv gravimeter, that has a resolution of 5 µGal and a standard deviation of less than 10 µGal. The elevation, latitude, and longitude were recorded at each site using a high-precision Trimble GPS unit and Geotrim VRS-GPS service that provides elevation accuracy less than 5 cm. Two local base stations were used for applying drift correction on the daily data. Magnetic surveys were carried out along both lines with the sampling distance of about 10 m, an adequate representation of the shortest significant spatial variation. Magnetic surveys were carried out using a Geometrics G858 magnetometer, which has a sensitivity of 0.01 nT.

The relative gravity readings were tied with the absolute gravity values of the first order gravity net of Finnish Geodetic Institute (FGI) using the nearest point next to Iisalmi church (*Kääriäinen,* 1997). Before the gravity data could be used to assess geol-

ogy, the measurements were also corrected for altitude variations (free-air correction) and the mass between the measurement point and sea level (Bouguer correction). Terrain correction was also made to account for topography variations near each observation point.

In addition to magnetic and gravity data, density and magnetic susceptibility were determined by petrophysical measurements from 66 rock samples collected in the study area (Fig. 2). The rocks were migmatites, granodiorites, granites, paragneisses, and their sheared counterparts. The new petrophysical data were combined with the existing GTK data (*Puranen et al.,* 1968; *Korhonen et al.,* 1989, 1993, 1997) to constrain gravity and magnetic modelling. Densities in the Iisalmi area ranged from 2600 kg/m^3 (granite) to 3200 kg/m^3 (metagabbro) with an average of 2730 kg/m^3, typical of many igneous rocks. The magnetic susceptibilities in the Iisalmi area have wider range between 0.005-0.1 SI. The high susceptibilities in the study area were primarily due to the higher percentage of ferromagnetic minerals, while relatively low susceptibility values suggest the destruction of magnetite due to the shearing process.

The MT soundings were carried out at 19 sites along an E-W directed profile as close as possible to the gravity line A. Broad-band instruments developed in the University of Uppsala and Oulu (*Smirnov et al.,* 2008) were used for measurements. The time variations of natural electric and magnetic fields were recorded in two orthogonal directions in addition to the vertical magnetic field. The magnetic field variations were measured with three induction coil magnetometers (MFS05-coils from Metronix) while the electric field was measured with two perpendicular electric dipoles (Pb/PbCl electrodes). The dipole length was about 100 m. The MT data were recorded at each site using two sampling frequencies: 20 and 1000 Hz simultaneously for one to two days. The length of the MT profile is c. 23 km with the distance between the sites varying from 500 to 1000 m depending on the existence of suitable space for installing the instruments and keeping them away from man-made electrical noise sources. All the data were processed with a robust remote reference code developed by Smirnov (2003). Remote reference data were obtained from a continuously recording instrument at a site close to Skellefteå, Sweden. The recorded time-series data were transformed to frequency domain and processed to determine the complex valued impedance tensors, the components of which relates measured electric and magnetic fields and can be expressed in terms of apparent resistivity and impedance phase at each site and at each frequency (period).

5   *Modelling of field data*

2.5-dimensional forward models were applied on the gravity and magnetic profile data using a ModelVision v. 12.0 software. ModelVision allows building geometric density and susceptibility geological models and comparing simulated responses with the field data. The purpose is to create a model that minimizes the difference between the measured field and observed data for geometrical and petrophysical properties (density and magnetic susceptibility) while acknowledging the known geological structures.

5.1   Modelling of gravity data

There are many appropriate algorithms for modelling gravity data. The majority of the existing algorithms assume that the density above the basement interface is uniform, allowing the use of constant-density modelling schemes (*Bhattacharyya and Navolio,* 1975). The change in geology and the difference of density values at various depths should be taken into consideration in the modelling. Gravity data was interpreted using 2.5-D density model that describes a 4000-m deep section of the upper crust below two profiles in the Iisalmi area. The forward model was made using polygonal bodies. The position, shape, dimensions, and density contrast were adjusted to get the best fit between the observed and calculated data. The amplitude of the gravity anomaly is proportional to the difference between its density and the background density while the shape of an anomaly depends essentially on the size and shape of the related source structures. The background density value (2730 kg/m3) was chosen based on the density of paragneisses in the study area. The regional field was set manually based on the regional Bouguer data (Fig. 4a).

Comparison of the regional Bouguer gravity with the geological map showed a close correlation between gravity anomalies and surface geology, whereas the gravity profile along line A showed two distinctive peaks in the gravity measurements (Fig. 8). The positive gravity anomaly (+3mGal) in the east is associated with dense migmatite (2770 k/gm^3). The wide negative gravity anomaly (-6mGal) is attributed largely to a low-density granodiorite (2680 k/gm^3). Steep gradients in the gravity profile occur where the composition changes from granodiorite to paragneiss. The dip between the main units is nearly vertical. The strike length of these two main bodies is about 20 km.
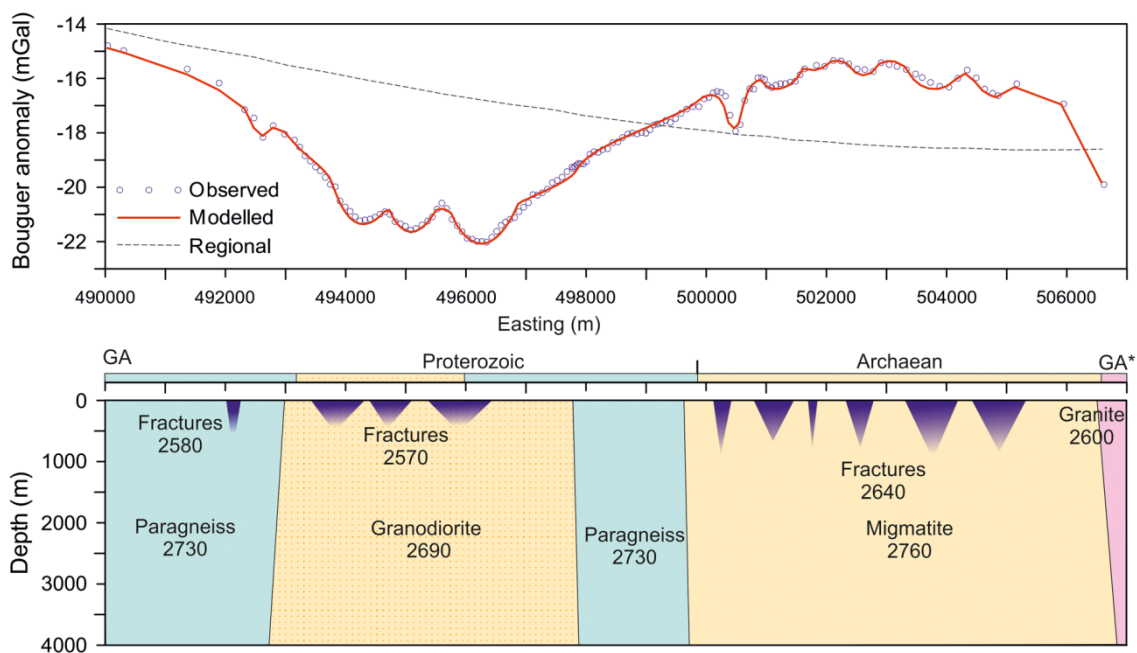

Fig. 8. 2.5-dimensional gravity model for line GA-GA* (Fig. 2). Numbers in the cross-section denote model densities in kg/m3. The stripe above the cross-section shows the surface lithology (Fig. 3) derived from the Geological map of Finland in a scale of 1:200000 © Geological Survey of Finland 2013 (Fig. 2).

The rapid negative gravity anomaly at the eastern end of the profile is due to granitic unit (2550 kg/m^3) that is partially outside the profile. The nine small wavelength anomalies are caused by near-surface density variations related to shear zones and fractures. To model the downward increasing density of the fracture zones we represented them as inverted triangles. The shear zones have a strike length of about 5 km and their density contrast with their host rock is about -100 kg/m3. Line B located about 5 km north to line A is shorter (6 km) and corresponds to the sloping part of the gravity anomaly in the middle of line A (Fig. 9). The fit between the observed and modelled data in line B results from extending polygonal bodies and fractures modelled in line A. Fig. 10 shows the outlines of the top surface of the interpreted density model along lines A and B on top of the geological map on the scale of 1:200.000.

Correlation of the Bouguer anomaly (Fig. 4) with the in-phase and quadrature components of the AEM data and the apparent resistivity data (Fig. 7) along profiles A and B indicates that the small-wavelength negative gravity anomalies are associated with conductors located at shallow depths. This suggests that the causative bodies of the negative gravity anomalies are related to water-filled fractures causing the reduction of the density (by 120-150 kg/m^3) and increase in the conductivity (by 0.001-0.002 S/m) compared to host rocks.
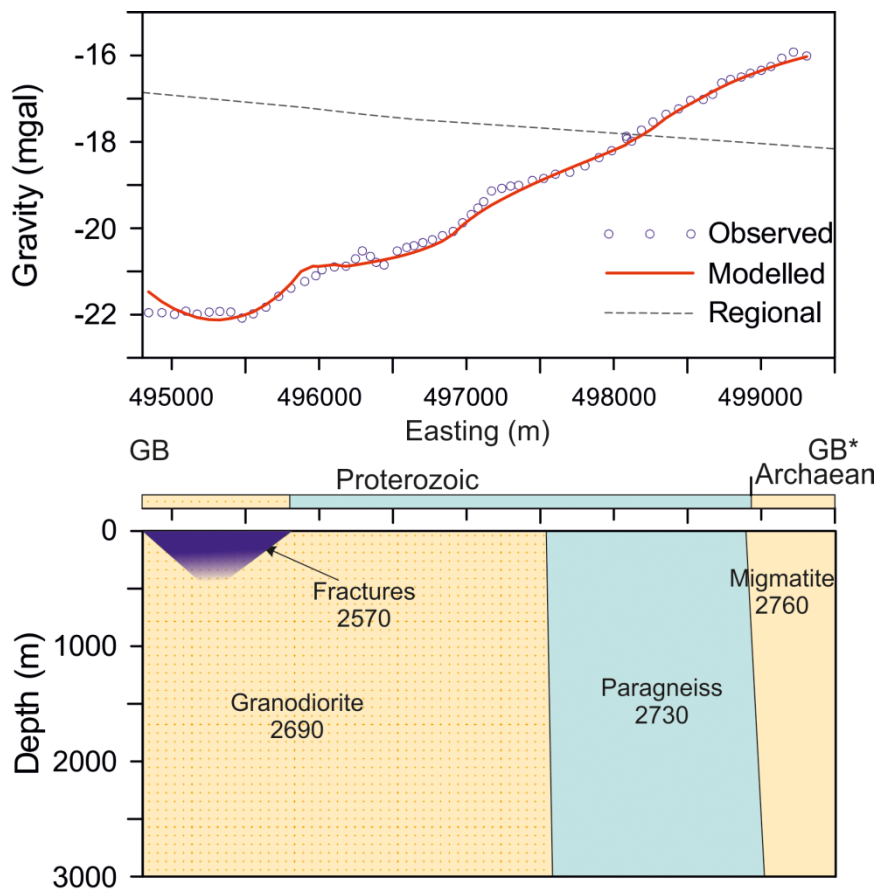

Fig. 9. 2.5-dimensional gravity model along the line GB-GB* (Fig. 2). Numbers in the cross-section denote model densities in kg/m3. The stripe above the cross-section shows the surface lithology (Fig. 3) derived from the Geological map of Finland in a scale of 1:200000 © Geological Survey of Finland 2013 (Fig. 2).
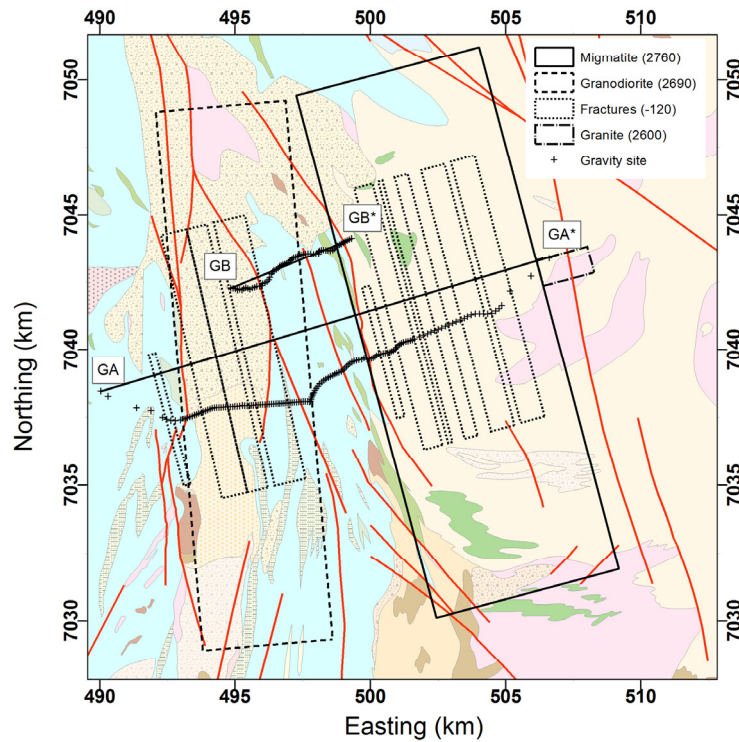
Fig. 10. Map of the density model for gravity lines GA-GA* and GB-GB* (Fig. 2). Rectangles denote the top surface of the density models. Crosses represent the location of gravity sites. The background map is the geological map on the scale of 1:200000 © Geological Survey of Finland 2013. The densities of three bodies (granodiorite, migmatite and granite) and the density contrast of the ten fractures of the model, given the in legend, are in kg/m^3.

5.2   Modelling of ground magnetic data

We performed forward modelling on the magnetic data to describe a 2500-m deep section of the upper crust using tabular bodies. The position, size, orientation, and magnetic susceptibility of the bodies were adjusted to get the best fit between the observed and calculated data. The intensity, inclination, and declination of the local geomagnetic field were set as 52500 nT, 75.3°, and 9.8°, respectively. The background was assumed non-magnetic.

The 2.5-dimensional modelling of the magnetic data explains the magnetic signature of the shear zones in the Iisalmi area (Fig. 11). The magnetic response of the shear zone looks more intensive and has more irregular variations than those of gravity data. The result consists of a number of parallel bodies with susceptibility contrasts varying between 0.005-0.08 SI, dip slightly to the east (82°), and the same general strike in NW-SE direction as in gravity data. Use of near-vertical tabular bodies gives the best fit between the observed data and calculated magnetic field. The structure is interpreted as sheared rocks striking NW-SE cutting through the area of transition between the Archaean and Proterozoic bedrocks. Outside the area of the line A, both on the Proterozoic side in west and on the Archaean side in east, the spatial magnetic field variations are negligible. Comparison of Figs. 3 and 11 shows that most of the magnetic anomalies

coincide with the Archaean-Proterozoic boundary that did not show any gravity signatures. This indicates that shearing has increased magnetic susceptibility within the Archaean-Proterozoic transition area. The western part of the line A, far from the Archaean-Proterozoic transition, is not showing any signature on shearing.
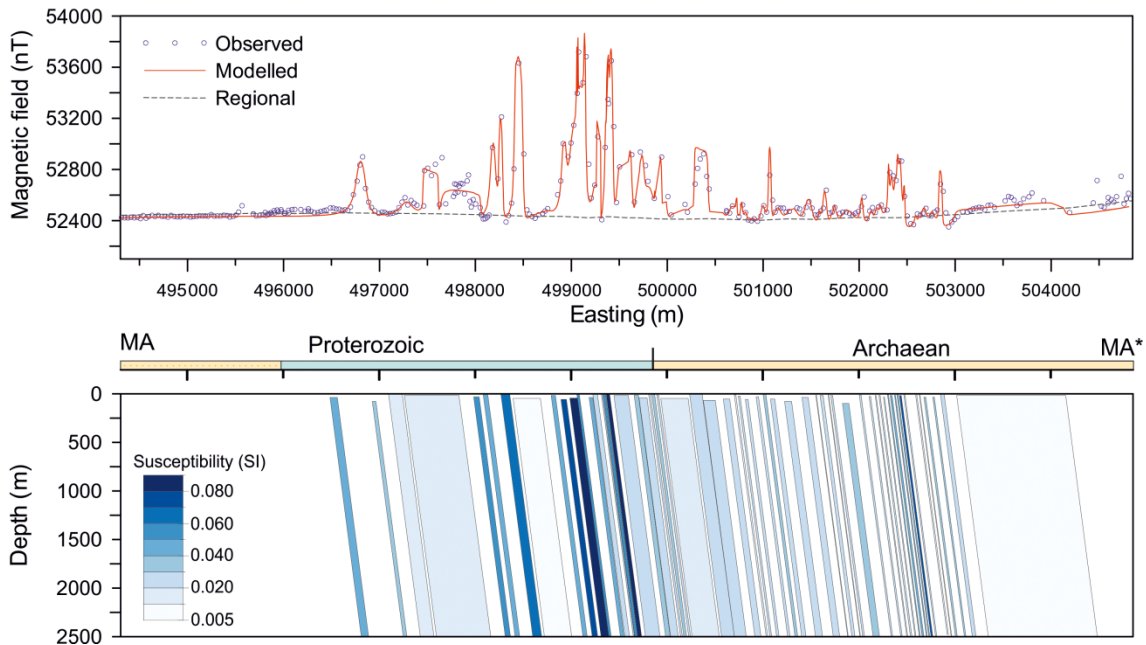

Fig. 11. 2.5-dimensional magnetic model along line MA-MA* (Fig. 2). Magnetic field intensity of 52500 nT, inclination of 75.3° and declination of 9.8° were used in the modelling. The stripe above the cross-section shows the surface lithology derived from the Geological map of Finland in a scale of 1:200000 © Geological Survey of Finland 2013 (Fig. 2).

5.3   Analysis and 2-D inversion of magnetotelluric data

MT method uses the Earth's natural electromagnetic field to investigate the subsurface geoelectrical structure. Dimensionality and strike analyses were done for the MT data to provide information about the dimensionality and regional strike direction of the subsurface structure (*Swift,* 1967; *Zhang et al.,* 1987; *Bahr,* 1988, 1991; *Smirnov & Pedersen,* 2009). Brief examples of structural-dimensionality of field data are provided by *Bahr* (1991) and *Eisel and Bahr* (1993). The results of these analyses were used to verify region for which 2-D inversion is justified. For example; the 3-D/2-D Bahr skew at most periods along the profile is generally below the upper limit of 2-D regional structure. The regional geoelectric strike direction of N20W, identified from the analyses of MT data, is consistent with the structural data having a dominant geological strike in a NNW-SSE direction. The determinant average (*Berdichevsky and Dmitriev*, 1976) of the impedance tensor data were inverted using the REBOCC code (*Siripunvaraporn and Egbert,* 2000) modified for the determinant inversion by *Pedersen and Engels* (2005). Use of the determinant allows to increase the amount of measured data usable for 2-D inversion and reduce the 3-D distortion effects in the MT responses (*Berdichevsky and Dmitriev,* 1976). The MT inversion was done along profile striking N70E

perpendicular to the regional strike direction and all sites were projected on it. A homogeneous half-space having a resistivity of 100 Ωm was used as initial model.

Fig. 12 displays the obtained model for the uppermost crust (0-10 km) together with the conductance of the model. The conductance is expressed as $S = \int_{h_1}^{h_2} \sigma(z)dz$, where $\sigma(z) = 1/\rho(z)$ (Sm^{-1}) is the conductivity at the depth z, ρ (Ωm) is resistivity and h_1 and h_2 are depth limits along the profile (0 and 10 km here). The final RMS error equals 0.77. We have limited the conductivity model to the depth of 10 km although the data ($T_{max} = 1000$ s) allows much greater penetration. First, we are interested in the upper crust and second, as the profile is rather short (23 km), in the deeper parts the model therefore becomes essentially 1-D. The entire area along the profile is highly resistive (> 1000 Ωm or even > 10000 Ωm in large parts of the model) with some less resistive near-surface bodies. Due to lateral resolution (site distance 500-1000 m), the exact location of these is questionable: they can be due to conductive rocks / fractured shear zones right beneath the site but also due to similar bodies between the sites. Deeper conductor (100–1000 Ωm) is detected in the western part of the profile. It dips westward and is likely imaged on the apparent resistivity map transformed from airborne electromagnetic data (Fig. 7d). Tests (not reproduced here) show that this conductor is required by data but its geometry and depth extent cannot be resolved.

6   *Discussion and geological interpretation*

The RLSC is a major crustal structure, spanning over a zone of a few tens of kilometres wide, in Central Finland separating the Archaean Karelian Province in the northeast from the Proterozoic Svecofennian Province in the southwest. Regional gravity and aeromagnetic data (Fig. 3) show a clear large-scale SE-NW directed trend along RLSC. In the Iisalmi area, to the east of the main gravity minimum (Fig. 3A; D4 & D5 in Fig 1), there is a weaker NS directed gravity minimum, which coincides with geological structural features (Fig. 3A; D2 & D3 in Fig. 1). The linear arrangement of aeromagnetic anomalies at the Archaean-Proterozoic boundary is related to magnetized rocks of the Outokumpu assemblage that gently dips southeast (*Airo et al.,* 2007). Sharp variations of magnetic highs correspond to a steep gradient on gravity and mark the transition from the Archaean to Proterozoic bedrock. Westward on the Proterozoic side and eastward on the Archaean side, the magnetic field variations are minor.

Modelling of ground gravity data shows that the large gravity minimum is caused by mostly unexposed granodiorites of low density while the gravity maxima to the east is corresponding with migmatites (Figs. 8 & 9). A sharp, steep gradient of about 5 mGal in the gravity profiles occurs where the profiles change from low-density granodiorite to high-density paragneiss rocks. Sharper minima are caused by fractured and sheared rocks. The contact between the Archaean and Proterozoic rocks is nearly vertical (Figs. 8 & 9). No estimate is found for the depth extent. On the other hand, modelling of ground magnetic data shows that magnetic anomalies exist mostly within the Archaean-Proterozoic (A-P contact) transition zone, which is affected by shearing; with stronger anomalies in its Proterozoic part, in particular (Fig. 11). The high amplitude of magnetic

anomalies suggests the presence of magnetite. Testing the gravity and magnetic models using different dips of bodies indicates that 82° eastward dip gives the best fit to the observed magnetic data. Furthermore, the dip angle of magnetic sources is steeper than the A-P contact found from gravity interpretation. This suggests that shearing cuts preexisting lithological units delineated by gravity modelling; in particular, the Archaean migmatites and Proterozoic paragneisess.
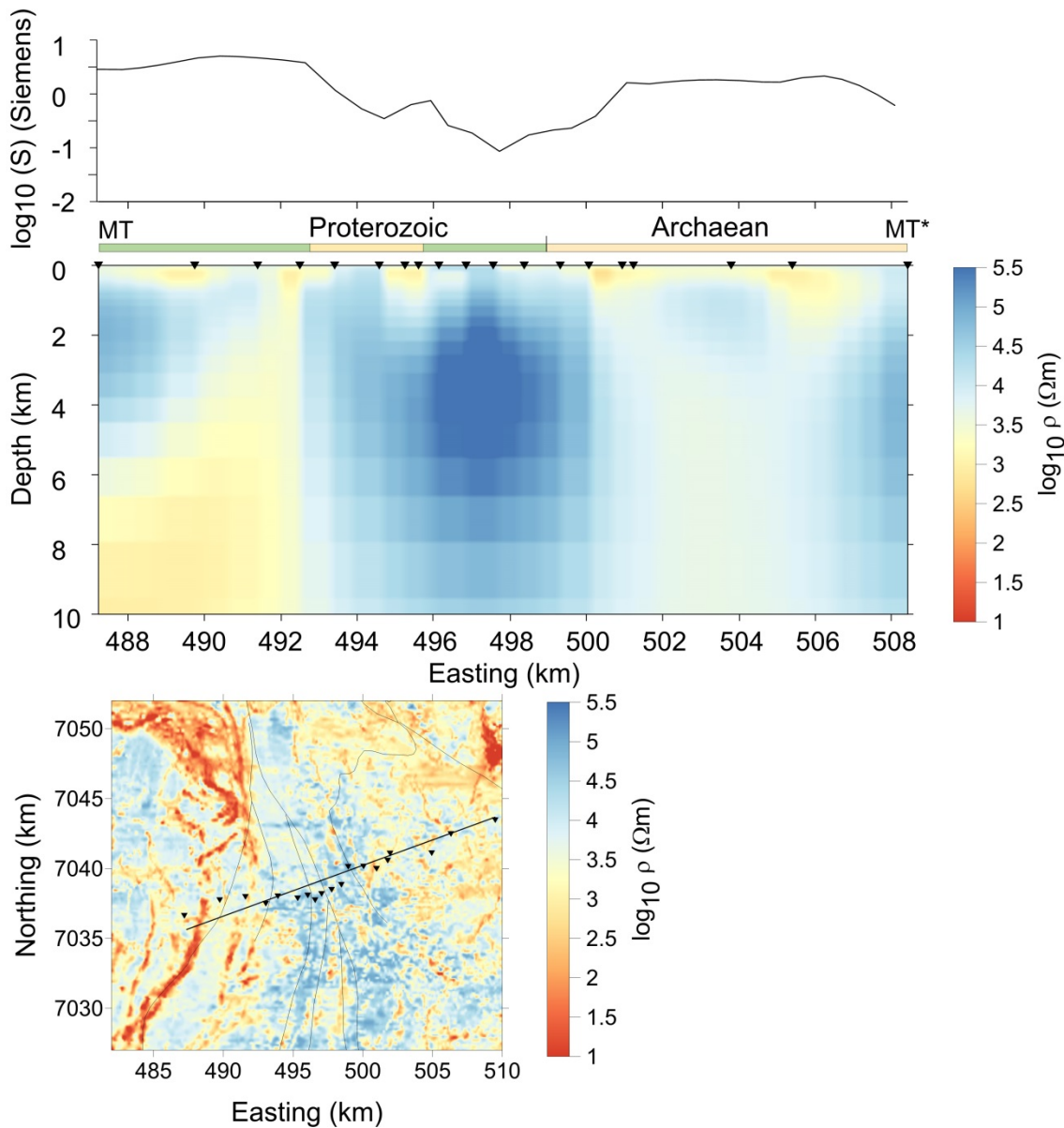

Fig. 12. A resistivity model from 2-D inversion of determinant MT data along line MT-MT* (Fig. 2). The inverted triangles show the location of the sounding sites. The uppermost graph shows the $\log_{10}$ conductance (in Siemens) integrated from surface to the depth of 10 km. The lowermost map shows the location of MT sites (inverted triangles) on the apparent resistivity of the basement derived from the joint inversion of airborne EM and magnetic data (Pirttijärvi et al., 2014). The straight black line denotes the resistivity model profile in the direction of N70E, perpendicular to the estimated geoelectric strike of N20W. Thin black lines denote structural lines from 1:1million map © Geological Survey of Finland 2009. The stripe above the cross-section shows the surface lithology derived from the Geological map of Finland in a scale of 1:200000 © Geological Survey of Finland 2013 (Fig. 2).

The upper crust in the Iisalmi area is rather resistive (> 1000 Ωm) on both the Archaean and the Proterozoic sides at least to the depths of 10 km. The total conductance of the first 10 km is around 1 Siemens or below as seen in the top panel in Fig. 12. This is in general very low value as the highest S-values of the crust (0–60 km) encountered in the Fennoscandian Shield exceed 20000 S (*Korja et al.,* 2002). The near-surface resistivity stemming in particular from the airborne electromagnetic data, however, shows some correlation with both gravity and magnetic anomalies. The MT profile, conducted across the Archaean-Proterozoic boundary, shows the existence of a moderately conducting feature in the western end of the profile. It dips westward and coincides with the near-surface conductors mapped by airborne electromagnetic data. These conductors are caused by the existence of thin and very conducting graphite- and sulphide-bearing rocks within otherwise highly resistive rocks as show in in Fig 12 (lowermost panel) according to surface lithology here as well as elsewhere in the Fennoscandian Shield. See more detailed discussions, e.g. in *Korja and Hjelt*, 1993 and *Korja et al.,* 2002.

High resistivity of the strongly sheared crust suggests the old shear complexes are not necessarily conductive opposite to many active shear complexes worldwide such as, for example, Fraser River Fault (Jones et al., 1992), San Andreas Fault (*Unsworth and Bedrosian*, 2004) and Red Sea Transform (*Maercklin et al.,* 2005). In most cases, the enhanced conductivity is explained by fluids flowing in the shear systems. However, it should be noted that graphite precipitation during the shearing process may leave stable conducting features that may be detectable by MT (Upton and Graw, 2008). The graphite precipitation should not be mixed with the shearing of carbon bearing sediments for which the shearing and metamorphism enable formation of conductive pathways. A good example comes from the Lapland Granulite Belt (*Korja et al.,* 1996), where it was observed that carbon bearing sediments become conductive in the shearing process but left non-sheared metasedimentary assemblages resistive.

7   Conclusions

Airborne and ground-based geophysical (gravity, magnetic and magnetotelluric) studies were joined to delineate the RLSC in the Iisalmi area. The shear zone in the area was outlined as a linear NW-SE trend of the Bouguer anomaly gradient at the transition from the Archaean Karelian Province to the Palaeoproterozoic Svecofennian Province. This is compatible with the aeromagnetic data, which reveal that the shear zone represents a broader area of NW-trending high-amplitude magnetic anomalies. The airborne electromagnetic and magnetotelluric data showed a generally highly resistive upper crust (up to 10 km) overprinted by several near-surface conductive anomalies striking NW. These conductors are due to the existence of graphite-bearing metasedimentary rocks at the western part of the study area and possibly shallow water-filled fractured shear zones in the central and eastern part. Modelling of the ground gravity survey data in the Iisalmi area suggested that the negative gravity anomalies of small wavelength are caused by near-surface density variations related to shear zones and fractures, but the depth extent and dip could not be resolved. However, according to magnetic model-

ling, the shear zone has a strong magnetic signature consisting of many near-vertical (82° eastward dip) sheet-like bodies with a greater depth extent (> 2 km) striking NW-SE.

References

Airo, M.-L., 1999. Aeromagnetic and petrophysical investigations applied to tectonic analysis in the northern Fennoscandian shield. Geologian tutkimuskeskus, Tutkimusraportti – *Geological Survey of Finland, Report of Jnvestigation* **145**. 51 pages.

Airo, M.-L. (ed.), 2005. Aerogeophysics in Finland 1972–2004: Methods, System Characteristics and Applications. *Geological Survey of Finland Special Paper*, **39**, 197 pages.

Airo, M.-L., T. Elbra, L. Kivekäs, T. Laine, M. Leino, S. Mertanen, L. Pesonen, S. Vuoriainen and H. Säävuori, 2007. Petrophysical laboratory measurements of the Outokumpu deep drill core samples. In: Kukkonen, I. T. (Ed.) *Outokumpu Deep Drilling Project, Sec. International Workshop, May 21–22, 2004, Espoo, Finland. Programme and Extended Abstracts.* Geological Survey of Finland, unpublished report **Q10.2/2007/29**, 35–40.

Airo, M.-L., E. Hyvönen, J. Lerssi, H. Leväniemi and A. Ruotsalainen, 2014. Tips and tools for the application of GTK's airborne geophysical data. *Geological Survey of Finland, Report of Investigation*, **215**, 33 pages.

Bahr, K., 1988. Interpretation of the magnetotelluric impedance tensor: regional Induction and local telluric distortion. *J. Geophys*, **62**, 119–127.

Bahr, K., 1991. Geological noise in magnetotelluric data: a classification of distortion types. *Phys. Earth planet. Inter.*, **66**, 24–38.

Berdichevsky, M.N. and V.I. Dmitriev, 1976. Basic principles of interpretation of magnetotelluric sounding curves, in Ádám, A. (Ed.) *Geoelectric and geothermal studies,* pp 165–221, ed., KAPG Geophysical Monograph, Akadémiai Kiadó.

Beaumont, C., R.A. Jamieson, M.H. Nguyen, and B. Lee, 2001. Himalayan tectonics explained by extrusion of a low-viscosity crustal channel coupled to focused surface denudation. *Nature*, **414**, 738–742.

Bhattacharyya, B.K. and M.E. Navolio, 1975. Digital convolution for computing gravity and magnetic anomalies due to arbitrary bodies. *Geophysics*, **40**, 981–992.

Blakely, R.J., 1995. Potential theory in gravity and magnetic applications. *Cambridge University Press*, 441 p.

Eisel, M. and K. Bahr, 1993. Electrical anisotropy in the lower crust of British Columbia: an interpretation of a magnetotelluric profile after tensor decomposition. *J. Geomag. Geoelectr.*, **45**, 1115–1126.

Ekdahl, E., 1993. Early Proterozoic Karelian and Svecofennian formations and the evolution of the Raahe-Ladoga ore Zone, based on the Pielavesi area, central Finland. *Geological Survey of Finland, Bulletin* **37**3.

Gaal, G. and R. Gorbatschev, 1987. An outline of the Precambrian evolution of the Baltic Shield. *Precambrian Res.*, **35**, 15–52.

Grad, M., T. Tiira and ESC Working Group, 2009. The Moho depth map of the European Plate. *Geophys.J.Int.*, **176**, 279–292, doi:10.1111/j.1365-246X.2008.03919.x.

Hautaniemi, H., M. Kurimo, J. Multala, H. Leväniemi and J. Vironmäki, 2005. The "Three In One" aerogeophysical concept of GTK in 2004. In: Airo, M-L. (Ed.), *Aerogeophysics in Finland 1972–2004: Methods, System Characteristics and Applications*. Geological Survey of Finland, Special Paper **39**, 21–74.

Jones, A.G., R.D. Kurtz, D.E. Boerner, J.A. Craven, G.W. McNeice, D.I. Gough, J.M. DeLaurier and R.G. Ellis, 1992. Electromagnetic constraints on strike-slip fault geometry —The Fraser River fault system. *Geology,* **20 (6):** 561–564. DOI: https://doi.org/10.1130/0091-7613(1992)020<0561:ECOSSF>2.3.CO;2.

Kärki, A., K. Laajoki, and J. Luukas, 1993. Major Palaeoproterozoic shear zones of the central Fennoscandian Shield. *Precambrian Research*, **64,** 207–223.

Koistinen, T., M.B. Stephens, V. Bogatchev, Ø Nordgulen, M. Wennerström and J. Korhonen (comp.), 2001. Geological map of the Fennoscandian Shield, scale 1:2 000 000. *Geological Survey of Finland, Special Maps* **48**.

Korhonen, J., H. Säävuori, H. Hongisto, P. Turunen, L. Kivekäs, T. Tervo, E. Lanne and A. Tuomi, 1989. Regional petrophysical program for Finland 1980–1991. In: Autio, S. (ed.) Geological Survey of Finland, Current research 1987–1988. *Geological Survey of Finland, Special Paper* **10,** 137–141.

Korhonen, J., H. Säävuori, M. Wennerström, L. Kivekäs, H. Hongisto and S. Lähde, 1993. One hundred seventyeight thousand petrophysical parameter determinations from the regional petrophysical Programme. In: Autio, S. (ed.) Geological Survey of Finland, Current Research 1991–1992. *Geological Survey of Finland, Special Paper* **18**, 137–141.

Korhonen, J.V., S. Aaro, J.-R. Skilbrei, R. Vaher and L. Zhdanova, 1997. Fennoscandian Magnetic Anomaly Data Base (1997) on a 1 km x 1 km grid, in: Boström, R., T. Carozzi, I. Arlefjärd and A.-S. Wahlberg (Eds.), *IAGA 1997 Abstract Book.*

Korhonen, J.V., S. Aaro, T. All, S. Elo, L.Å. Haller, J. Kääriäinen, A. Kulinich, J.R. Skilbrei, D. Solheim, H. Säävuori, R. Vaher, L. Zhdanova and T. Koistinen, 2002a. Bouguer Anomaly Map of the Fennoscandian Shield 1:2 000 000. *Geological Surveys of Finland, Norway and Sweden and Ministry of Natural Resources of Russian Federation.*

Korhonen, J.V., S. Aaro, T. All, H. Nevanlinna, J.R. Skilbrei, H. Säävuori, R. Vaher, L. Zhdanova and T. Koistinen, 2002b. Magnetic Anomaly Map of the Fennoscandian Shield 1:2 000 000. *Geological Surveys of Finland, Norway and Sweden and Ministry of Natural Resources of Russian Federation.*

Korja, A., T. Korja, U. Luosto, and P. Heikkinen, 1993. Seismic and geoelectric evidence for collisional and extensional events in the Fennoscandian Shield – implications for Precambrian crustal evolution. *Tectonophysics*, **219**, 129–152.

Korja, A., R. Lahtinen, P. Heikkinen, I.T. Kukkonen, and FIRE Working Group, 2006. A geological interpretation of the upper crust along FIRE 1. Pp. 45–76 in Kukkonen, I.T and Lahtinen, R. (ed.), 2006. Finnish Reflection Experiment FIRE 2001–2005. *Geological Survey of Finland, Special paper* **43**, 247 pp.

Korja, A., P. Kosunen, and P.J. Heikkinen, 2009. A Case Study of Lateral Spreading the Precambrian Svecofennian Orogen In: Ring, U. and Wernicke, B. Extending a Continent: Architecture, Rheology and Heat Budget. *Geological Society of London, Special Paper* **321**, 225–251. DOI: 10.1144/SP321.11.

Korja, A., O.T. Rämö, O. Eklund, T. Korja, A. Kärki and P. Hölttä. 2012. Evolution of the middle crust in Central Fennoscandia – MIDCRUST. Pp. 39–42 in Kukkonen, I.T., Kosunen E.M., Oinonen, K., Eklund, O., Korja, A., Korja, T., Lahtinen, R., Lunkka, J.P. and Poutanen, M., 2012 (Eds.). Lithosphere 2012 – Seventh Symposium on the Structure, Composition and Evolution of the Lithosphere in Finland. Programme and Extended Abstracts, Espoo, Finland, November 6–8, 2012. *Institute of Seismology, University of Helsinki, Report* **S-56**, 116 pages.

Korja, T., P. Zhang, and K. Pajunpää, 1986. Magnetovariational and magnetotelluric studies of the Oulu-anomaly on the Baltic Shield Finland. *Journal of Geophysics*, **59**, 32–41.

Korja, T. and S.-E. Hjelt, 1993. Electromagnetic studies in the Fennoscandian Shield – electrical conductivity of Precambrian crust. *Phys. Earth Planet. Int.*, **81**, 1–4, 107–138.

Korja, T. and K. Koivukoski, 1994. Magnetotelluric investigations along the SVEKA profile in central Fennoscandian Shield, Finland. *Geophys. J. Int.*, **116**, 173–197.

Korja, T., P. Tuisku, T. Pernu, and J. Karhu, 1996. Lapland Granulite Belt – implications for properties and evolution of deep continental crust. *Terra Nova*, **8**, 48–58.

Korja T., M. Engels, A.A. Zhamaletdinov, A.A. Kovtun, N.A. Palshin, M.Yu. Smirnov, A. Tokarev, V.E. Asming, L.L. Vanyan, I.L. Vardaniants, and BEAR Working Group, 2002. Crustal conductivity in Fennoscandia – a compilation of a database on crustal conductance in the Fennoscandian Shield. *Earth Planets Space*, **54**, 535–558.

Korja, T., 2007. How is the European Lithosphere Imaged by Magnetotellurics? *Surv. Geophys*., **28**, 239–272, DOI 10.1007/s10712-007-9024-9.

Korsman, K., T. Korja, M. Pajunen, P. Virransalo and GGTSVEKA Working Group, 1999. The GGT/SVEKA transect: structure and evolution of the continental crust in the Paleoproterozoic Svecofennian orogen in Finland. *International Geology Review,* **41**, 287–333.

Kukkonen, I.T and R. Lahtinen, R. (ed.), 2006. Finnish Reflection Experiment FIRE 2001–2005. *Geological Survey of Finland, Special paper* **43**, 247 pp.

Lahti, I., T. Korja, L.B. Pedersen, and BEAR Working Group, 2002. Lithospheric conductivity along GGT/SVEKA Transect: implications from the 2-D inversion of magnetotelluric data, in Lithosphere 2002, Second Symposium on the Structure, Composition and Evolution of the Lithosphere in Finland, pp. 75–78, ed. Lahtinen et al., *Institute of Seismology, University of Helsinki, Report* **S-42**.

Lahtinen, R., A. Korja, and M. Nironen, 2005. Paleoproterozoic tectonic evolution. In: Lehtinen, M., Nurmi, P. and Rämö, O.T. (Eds.): *Precambrian Geology of Finland – Key to the Evolution of the Fennoscandian Shield.* Elsevier B.V., Amsterdam, pp. 481–532.

Lanne, E., U. Väisänen, H. Forss, A. Ruotsalainen and J. Lehtimäki, 1998. Geophysical prospecting of bedrock aquifers in Finland. In: Casas, A. (ed.) *Proceedings of the IV Meeting of the Environmental and Engineering Geophysical Society (European section)*, September 14–17, 1998, Barcelona, Spain. Madrid: Instituto Geográfico Nacional, 159–162.

Lanne, E., J. Lehtimäki, H. Vanhala and U. Väisänen, 2002. Geophysical characteristics of Precambrian fracture zones – A case study from Rovaniemi, Northern Finland. *8th meeting, (EEGS-ES) Environmental and engineering geophysics, 8–12 September, 2002.* Proceedings, Aveiro Portugal, 4 p.

Leväniemi, H, D. Beamish, H. Hautaniemi, M. Kurimo, I. Suppala, J. Vironmäki, R.J. Cuss, M. Lahti and E. Tartaras, 2009. The JAC airborne EM system AEM-05. *Journal of Applied Geophysics,* **67**, 219–233.

Luosto, U., 1991. Moho depth map of Fennoscandian Shield based on seismic refraction data, in Structure and Dynamics of the Fennoscandian Lithosphere, pp. 43–49, eds. Korhonen, H. & Lipponen, A., *Report* **S-25**, Instit. Seism., Univ. Helsinki, Helsinki, Finland.

Maercklin, N., B.A. Bedrosian, C. Haberland, O. Ritter, T. Ryberg, M. Weber, and U. Weckmann, 2005. Characterizing a large shear-zone with seismic and magnetotelluric methods: The case of the Dead Sea Transform. *Geophys. Res. Lett.,* **32**, L15303, doi:10.1029/2005GL022724, 2005.

Neska, A., 2016. Conductivity Anomalies in Central Europe. *Surv. Geoph*., 37, 5–26.

Paavola J., 1991. Iisalmen kartta-alueen kallioperä. Summary: Pre Quatemary rocks of the Iisalmi map-sheet area. Explanation to the Maps of Pre-quaternary Rocks. Sheet 3341. *Geological Survey of Finland.*

Pedersen, L.B. and M. Engels, 2005. Routine 2D inversion of magnetotelluric data using the determinant of the impedance tensor. *Geophysics,* **70,** NO. 2, G33–G41, 10.1190/1.1897032.

Peltoniemi, M., 1982. Characteristics and results of an airborne electromagnetic method of geophysical surveying. *Geological Survey of Finland, Bulletin*, **321**. 229 p.

Peltoniemi, M., 2005. Airborne geophysics in Finland in perspective. In: Airo, M.-L. (Ed.), Aerogeophysics in Finland 1972–2004: Methods, System Characteristics and Applications. *Geological Survey of Finland, Special Paper,* **39**, pp. 7–20.

Pirttijärvi, M., 2012. FOURPOT, Processing and analysis of potential field data using 2-D Fourier transform, User's guide to version 1.3. *Department and Physics, University of Oulu*. pp. 54.

Pirttijärvi, M., M. Abdel Zaher and T. Korja, 2014. Combined inversion of airborne electromagnetic and static magnetic field data. *Geophysica*, **50(2)**, 65–87.

Poikonen, A., K. Sulkanen, M. Oksama and I. Suppala, 1998. Novel dual frequency fixed wing airborne EM system of geological survey of Finland (GTK). *Exploration Geophysics*, **29**, 46–51.

Puranen, M., V. Marmo and U. Hämäläinen, U., 1968. On the geology, aeromagnetic anomalies and susceptibilities of Precambrian Rocks in the Virrat region (Central Finland). *Geoexploration*, **6**, 163–184.

Puranen, R. and K. Sulkanen, 1985. Technical description of microcomputer-controlled petrophysical laboratory. Geological Survey of Finland, archive report, Ql5/27185/1. 252 p.

Siripunvaraporn, W. and G. Egbert, 2000. An Efficient Data-Subspace Inversion for Two Dimensional Magnetotelluric Data. *Geophysics*, **65**, 791–803.

Smirnov, M.Yu., 2003. Magnetotelluric data processing with a robust statistical procedure having a high breakdown point. *Geophys. J. Int.,* **152**, 1–7.

Smirnov, M., T. Korja, L. Dynesius, L.B. Pedersen and E. Laukkanen, 2008. Broadband magnetotelluric instruments for near-surface and lithospheric studies of electrical conductivity: A Fennoscandian pool of magnetotelluric instruments. *Geophysica,* **44(1–2),** 31–44.

Smirnov, M. Yu. and L.B. Pedersen, 2009. Magnetotelluric measurements across Sorgenfrei-Tornquist zone in southern Sweden and Denmark. *Geophys. J. Int.,* **176**, 443–456.

Swift, C.M., 1967. A magnetotelluric investigation of an electrical conductivity anomaly in the south-western United States, PhD thesis, *M.I.T., Cambridge*, MA, USA.

Telford, W.M., L.P. Geldart and R.E. Sheriff, 1978. Applied geophysics, First Edition, Cambridge, England. *Cambridge University Press*, 561 p.

Unsworth, M. and P.A. Bedrosian, 2004. On the geoelectric structure of major strike-slip faults and shear zones. *Earth Planets Space*, **56**, 1177–1184, 2004.

Unsworth, M., 2009. Magnetotelluric Studies of Active Continent–Continent Collisions. *Surv. Geophys.,* DOI 10.1007/s10712-009-9086-y.

Upton, P. and D. Craw, 2008. Modelling the role of graphite in development of a mineralised mid-crustal shear zone, Macraes mine. *New Zealand Earth and Planetary Science Letters,* **266** (2008) 245–255. doi:10.1016/j.epsl.2007.10.048.

Vaittinen, K., T. Korja, P. Kaikkonen, I. Lahti and M.Yu. Smirnov, 2012. High-resolution magnetotelluric studies of the Archaean-Proterozoic border zone in the Fennoscandian Shield, Finland. *Geophys. J. Int*., **188**, 908–924. doi: 10.1111/j.1365-246X.2011.05300.x.

Vanderhaeghe, O. and C. Teyssier, 2001a. Crustal-scale rheological transitions during late-orogenic collapse. *Tectonphysics*, **335**, 211–228.

Vanderhaeghe, O. and C. Teyssier, 2001b. Partial melting and flow of orogens. *Tectonophysics*, **342**, 451–472.

Woodard, J., P. Tuisku, A. Kärki, Y. Lahaye, J. Majka, H., Huhma, and M.J. Whitehouse, 2015. Temporal Evolution of the Raahe-Ladoga Shear Complex, Finland: Constraints from Zircon and Monazite Geochronology in the Pielavesi Shear Zone. Submitted to Precambrian Research.

Zhang, P., R.G. Roberts, and L.B. Pedersen, 1987. Magnetotelluric strike rules. *Geophysics,* **52**, 267–278.

Zhao, G.M. Sun, S.A. Wilde, and S. Li, 2004. A Paleo-Mesoproterozoic supercontinent: assembly, growth and breakup. *Earth Science Review,* **67**, 91–123.